Peptide-functionalized Polymeric Nanoparticles for Cancer Therapy Applications

Sílvia Catarina da Silva Lobo

MSc in Microbiology

Supervisors: Dr. Nuno Filipe Santos Bernardes and Dr. Karina Marangoni

Abstract

The work presented in this dissertation had as objectives studying the interaction that the p18 peptide conjugated with nanoparticles (NPs) had with lung cancer and non-cancer cells, and the impact that p28 peptide and NPs functionalized with p28 had in the plasma membrane order of lung cancer cells. Both peptides are a part of azurin, which is a protein that can enter human cancer cells and induce apoptosis. Firstly, it was proceeded the conjugation of p18 or p28 with PLGA-PEG-Mal in which the efficiency conjugation percentage was calculated through HPLC, and then the functionalized NPs were produced. For the experiment with p18, the cell-NP interaction of p18 functionalized and non-functionalized NPs was analyzed through flow cytometry. These results were compared with those obtained by previous studies of p28 and it was concluded that p18 does not interact more with cells than p28, therefore it does not bring more advantages than p28. For the second objective, a new experiment with PLGA-p28-NPs was made to study their effect at the level of plasma membrane organization of cancer cells, when these were incubated with functionalized NPs (250 µg/mL), non-functionalized NPs (250 µg/mL), Free p28 (2.5 µM), and Free p28 (50 µM). The evaluation was possible with the use of the fluorescent probe Laurdan and a two-photon excitation microscopy. Every condition appears to interfere with the fluidity of the plasma membrane order when compared to the control. Our preliminary data evidence that Free p28 (2.5 µM) was the treatment that caused the most membrane perturbation, reinforcing that p28 may lead to a decrease content of lipid rafts, which confers a higher membrane order and stability of cancer cells.

1. Introduction

Cancer is one of the primary diseases that threatens human lives and currently one of the principal treatments of cancer includes chemotherapy. However, chemotherapeutic drugs can cause harm to healthy cells of the human body, because they are nonspecifically distributed in the body, causing toxicity to the patient [1]. In recent years, nanotechnology has been studied and optimized to be used for cancer treatment. Nanotechnology is the science involved in the design, synthesis, characterization, and application of materials and devices whose smallest functional organization is on the nanometer (nm) scale [2]. So, this new field promoted the production of a nanosized material, which could be promising for the development of a new application for cancer treatment, and even for its diagnosis, because they are small enough to be able to penetrate eukaryotic cell membranes. These

nanosized materials are called nanoparticles (NPs).

NPs are nanocarriers that, in nanomedicine, became efficient for therapies due to its unique properties, such as drug delivery, because NPs can carry drugs inside and protect them from degradation, which promotes developments in the treatment of cancer [2]. NPs such as liposomes, polymeric nanoparticles, dendrimers macromolecules, quantum dots, and carbon nanotubes have been commonly used in cancer treatment [3,4]. Although NPs alone are a great new strategy for cancer therapy and offer a lot of advantages, their direction towards cancer cells is non-specific and the drug can get released out of the NP before it can enter the target cells. Consequently, one way to improve this specificity is by using cell-penetrating peptides (CPPs), which are positively charged short peptides with 5-30 amino acids long that can penetrate the biological membrane and deliver a variety of materials into cells. CPPs are ligands that are introduced onto the NP surface to target changes in cancer cell biology, which are upregulated in comparison to healthy cells [5].

A lot of studies have been made with NPs conjugated with CPPs on their surface for different cancer therapies. One of these innumerous studies worked with the CPP p28 (28 amino acids), which comes from the protein azurin. Azurin is a copper-containing redox protein secreted by *Pseudomonas aeruginosa* that contains 128 amino acids (aa) [6]. It has been reported that p28 peptide prefers to enter cancer cells rather than normal ones, because the membrane receptors that mediate p28 internalization often show higher expression levels in cancer cells compared to normal ones [7]. This peptide is localized in the alpha-helix region, within 50-77 aa, domain responsible for azurin's antiproliferative activity, and it is also characterized for being amphipathic, which means it has a hydrophilic domain (50-66 aa) localized in the C-terminal, and a hydrophobic domain (67-77 aa) localized in the N-terminal (Figure 1) [8–10]. Garizo *et al.* [11] utilized p28, with a cysteine in C-terminal, as a molecule for nanosized drug delivery systems and produced gefitinib (GEF)-loaded p28 functionalized poly (lactic-co-glycolic acid) (PGLA) NPs to target lung cancer cells. Therefore, the functionalization of this nanocarrier with p28 promotes an active tumor targeting strategy, accumulating into the tumor region, and subsequently binding to the target cells. It is known that the domain near N-terminal of p28 is responsible for the penetration capability in human cancer cells, and when entering the nucleus of these cells, p28 can bind to the DNA-binding domain of the tumor-suppressor protein p53, inhibiting its proteasomal degradation, which consequently promotes apoptosis [7]. A nanosystem (p28-NPs-GEF) was developed in which the p28 favored the internalization of the nanosystem in lung cancer cells, where GEF was released to exert its anticancer therapeutic activity. This nanosystem interacted with two human cell lineages, the A549 lung cancer cell line and 16HBE14o- bronchial non-cancer cell line [11]. According to their results, p28 improved the specific interaction of these NPs with A549 lung cancer cells. Furthermore, p28-NPs containing GEF were able to specifically lower the metabolic activity of A549 cells while having no effect on non-cancer cells. *In vivo* experiments, utilizing A549 subcutaneous xenografts, revealed that p28-NPs-GEF

decreased A549 primary tumor burden and the development of lung metastases. In summary, the progression of p28-functionalized NPs capable of penetrating cancer cell membranes, while delivering GEF, may provide a new strategy to improve lung cancer therapy [7].

Therefore, for the first objective of this work, we tested the interaction of repeated similar nanosystem, but with a change on the CPP that instead of being the p28 peptide we utilized a smaller version of that same peptide called p18 peptide (60-77 aa of azurin), which has the same origin as p28. The difference between these two peptides, despite being the size, is that p18 does not have the cytotoxicity domain present in the C-terminal region like p28 has, therefore it only has the domain responsible for the preferential entry into cancer cells present in the N-terminal region (Figure 1). The advantages would be working with a much smaller peptide which is cheaper, it has a lower risk of degradation, and, hypothetically, smaller molecules have a higher affinity/specificity to target, lower toxicity profiles, and also a better tissue penetration [124]. Therefore, one of the objectives of this thesis was to see if there were advantages in using a much smaller peptide in terms of the efficiency of the interaction of NP conjugated with the p18 peptide into both cancer and non-cancer cells of the human body.

Another objective of this work was to continue another experiment related to p28, and in this experiment, the impact that four different experimental conditions had at the level of the plasma membrane order in A549 cancer cells was evaluated. These four conditions were Free p28 (2.5 μM), Free p28 (50 μM), p28-NPs (250 μg/mL), which are called functionalized NPs (f-NPs), and NPs without p28 (250 μg/mL), which are called non-functionalized NPs (nf-NPs). This impact was assessed using a fluorescent probe called Laurdan (2-dimethylamino-6-lauroylnaphthalene) with a two-photon excitation microscopy.

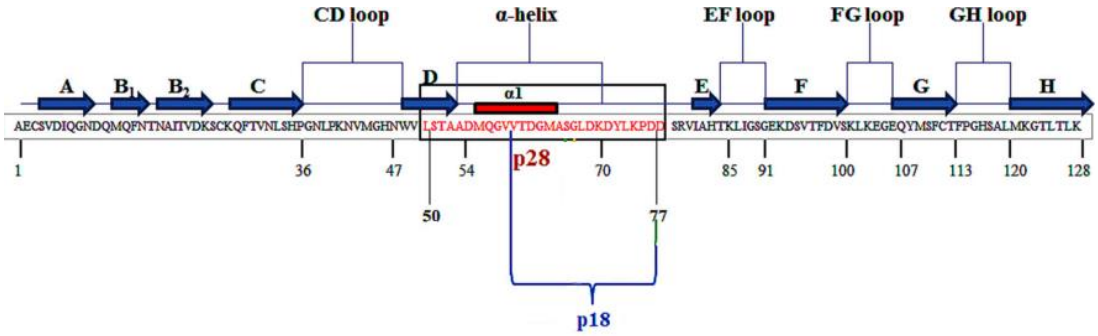

Figure 1 - Azurin's sequence (128 amino acids), in the black box is located the p28 peptide (28 amino acids) from amino acids 50-77, and from amino acids 60-77 it is located the p18 peptide. Source: Yaghoubi *et al.,* 2020 (doi: 10.3389/fonc.2020.01303).

2. Materials & Methods

2.1. Peptide Synthesis

p18 with a cysteine in the C-terminal (CLSTAADMQGVVTDGMAS-NH_2, 1756.02 Da) was synthetized and provided by CASLO ApS., LTD. at 98.7% purity percentage. p28 with a cysteine in the C-terminal (CLSTAADMQGVVTDGMASGLDKDYLKPDD-NH_2, 3017.29 Da) was synthetized and provided by CASLO ApS., LTD. at > 95% purity percentage.

2.2. Cell Culture and Growth Conditions

The A549 human lung cancer cell line, which was purchased from the European Collection of Authenticated Cell Cultures (ECACC), was used throughout this thesis. Cells were grown in Dulbecco's Modified Eagle Medium (DMEM; Gibco® by Life Technologies), supplemented with 10% heat-inactivated Fetal Bovine Serum (FBS; Gibco® by Life Technologies), 10,000 U/mL of penicillin, and 100 mg/mL of streptomycin (PenStrep, Invitrogen). These cells were chemically detached with 0.05% TrypLE™ Express (Gibco® by Life Technologies) and passed two to three times a week. The 16HBE14o- human bronchial non-cancer cell culture was used as a control cell line. It was cultured in Minimum Essential Medium (MEM) without Earls salts supplemented with 10% of FBS, 10000 U/mL penicillin, and 10000 mcg/mL streptomycin. This cell line was cultured in fibronectin-coated T-flasks. Both cancer and non-cancer cells were maintained at 37 ºC in a humidified environment with 5% CO_2 (Binder CO2 incubator C150), to preserve the pH of the growth medium.

2.3. Conjugation of p18-C or p28-C Peptide to PLGA-PEG-Mal

The interaction between maleimide (Mal) and the thiol (SH) group present in the cysteine (C-terminal) of the peptide was promoted in order to conjugate p18 or p28 to PLGA-PEG-Mal. First, 15 mg of PLGA-PEG-Mal was dissolved in 1 mL of N,N-dimethylformamide (DMF, CARLO ERBA) for an hour under soft agitation, 1.5 mg of tris(2-carboxyethyl) phosphine hydrochloride (TCEP, Aldrich) was dissolved in 1 mL of DMF, and the peptide was also dissolved in 1 mL of DMF during 15 minutes. 150 µL of TCEP was added to the peptide solution after 15 minutes, and the mixture was then gently stirred for a further hour at room temperature. The TCEP + peptide combination was then combined with the volume of PLGA-PEG-Mal solution, and the mixture was then agitated at 4 °C for 24 hours. The next day, the PLGA-PEG-Mal-peptide solution was precipitated two times with diethyl ether (Sigma-Aldrich®), 16 mL each time, and 3 times with ultrapure water (MilliQ station from Millipore Corporation), 5 mL each time, respectively. The water used is to dissolve the free peptide that precipitated with the polymer, and thus wash the pellet so that it is only constituted by the polymer PLGA-PEG-Mal-peptide. Following each precipitation, the pellet was sonicated (Ultrasonic Cleaner, Branson 200) for 3 minutes, centrifuged (Centrifuge 5840R, Eppendorf) for 5 minutes at 3300xg at 4 °C, and then the supernatant was collected and stored at -80 °C overnight. The pellet was lyophilized in a freeze dryer (ScanVac CoolSafe, LaboGene) the next day, and the amount of PLGA-PEG-Mal-peptide recovered was weighted. Lastly, the PLGA-PEG-Mal-peptide pellet was stored at -20 ℃.

2.4. Indirect Quantification by HPLC to Determine the Efficiency of PLGA-PEG-Mal-peptide Conjugation

The supernatants collected during the conjugation step were evaluated using a Hitachi LaChrom Elite® high-performance liquid chromatography (HPLC) System (Hitachi High Technologies America, Inc) to ascertain the percentage of conjugation of the peptide to PGLA-PEG-Mal. A LiChrospher® 100 RP-18 column (5 m, 4.6 x 250 mm) was used for the chromatographic separations, along with a LiChrospher 100 RP-18 guard column and stationary phase kept at 25 °C. Two acetonitrile buffers (2% CH3CN, Carlo Erba), 0.05% trifluoroacetic acid (TFA, Sigma), and ultrapure water made up the mobile phase. The detector was set at 220 nm and the HPLC equipment was configured for UV-Vis. Each sample was examined for 40 minutes while the flow rate was adjusted to 1 mL/min and the injection volume to 90 µL. A calibration curve for determining the peptides' concentration was performed under the same conditions (3, 6, 15, 45, 90, 125, 250, and 400 µg/mL dissolved in ultrapure water). To ensure that none of the reagents employed in the conjugation process interfered with the analysis, control samples DMF and TCEP were also run through the HPLC column used. To determine peptides' conjugation to the polymer, we determined how much of the peptide did not conjugate to the polymer using the supernatants of diethyl ether and ultrapure water precipitation steps. Finally, the EZChrom Elite software was utilized to calculate the area under the curve of each peak. To determine the peptide concentration at each sample from the precipitation steps, an equation for the calibration curve was first determined (Equation 1):

$$Area\ (Au) = a\ \times peptide\ concentration\ + b$$

(Equation 1)

After calculating the concentration of the peptide present in each supernatant, the final mass of the peptide ($m_{f\ peptide}$) was calculated to determine the conjugation efficiency percentage (CE%) with the value of the initial mass of the peptide ($m_{i\ peptide}$):

$$Conjugation\ Efficiency\ (CE;\ \%) = \left(\frac{mi\ peptide - mf\ peptide}{mi\ peptide}\right) \times 100$$

(Equation 2)

2.5. Production of PLGA Nanoparticles by Nanoprecipitation Method

Two types of NPs were made: non-functionalized NPs and functionalized NPs. The non-functionalized NPs do not have p18 or p28 exposed in their surface while functionalized NPs do. To produce non-functionalized NPs, 20 % PLGA-PEG-Mal, 10 % PLGA-FKR648 (fluorescent probe, only for cellular interaction), and 70 % (for cellular interaction) or 80% (for membrane order experiments) PLGA (50:50 LA:GA; 44 kDa, Purasorb® PDLG 5004A, Corbion) were combined, to a total of 20 mg of polymer. The same was used to produce functionalized NPs but instead of using PLGA-PEG-Mal, PLGA-PEG-Mal-p18C or PLGA-PEG-Mal-p28C were used. In each formulation, 3 mL of DMF (organic phase) were added to the polymers and left at room temperature overnight to a complete dissolution. In the next day, using a needle in a previously cut 1000 µL tip, the organic phase was slowly and steadily added into the aqueous phase containing 10 mL of Tween 80 1 % at pH 7.4 and each solution was kept under soft agitation for 3 hours to evaporate the organic solvent. After the NPs production, the washing step was carried out to remove the surfactant and elute the organic solvent that had not evaporated yet. This process was proceeded by using Amicon Ultra-15 Centrifugal Filter units (100 kDa) (Merk Millipore, UFC910024) and cleaned with ultrapure water combined with centrifugation at 600xg, 4 ℃, for 10 minutes. Lastly, the NPs colloidal solutions were collected into a microtube and stored at 4 ℃ until characterization through Zetasizer.

2.6. Characterization of Nanoparticles Using Zetasizer Software

The NPs were characterized by using the software Zetasizer which analyzes their average size (Z-average), polydispersity index (PDI) by dynamic light scattering (DLS) (0-1), and zeta-potential (ζ-potential) through Laser Doppler Anemometry (LDA), using a Malvern Zetasizer Nano ZS instrument (Malvern Instruments Ltd., Worcestershire, UK). Each sample (before and after the washing step) was diluted (1:100, v/v) with 10 mM NaCl pH 7.4, and the laser was set to a wavelength of 633 nm and left for stabilization for 20 minutes.

2.7. Cell-p18C Nanoparticles Interaction by Flow Cytometry

First, the preparation of the cell lines A549 lung cancer cells and 16HBE14o- human bronchial non-cancer cells was carried out to compare the cell uptake of the functionalized NPs and non-functionalized NPs. In total, eight 6-well plates were used, four for each cell line (one treated with functionalized NPs and the other with non-functionalized NPs with acid wash, the other two were without the acid wash). A 6-well plate is intended to have $5x10^5$ cells/well for the A549 lineage and $1x10^6$ cell/well for the 16HBE14o- lineage. All plates were put at 37 ℃ in an incubator overnight. On the following day, the treatment of functionalized and non-functionalized NPs was carried out in which the cells were washed with PBS 1x and treated with different concentrations of functionalized NPs and non-functionalized NPs (50, 100, 250, 500 µg/mL) with and without the acid wash. The wells were incubated for 4 hours, after which the cells were washed with phosphate buffer saline (PBS) twice and two 6-wells of each lineage (four 6-wells in total) were acid washed with a buffer composed of 0.5 M NaCl, 0.2 M acetic acid at pH 3 (dissolved in MilliQ Water). Then, cells were detached using TrypLE™ Express before being incubated for 2 minutes. After this time, 1 mL of medium was placed in each well to neutralize the effect of the TrypLE™. Then, the contents of each well were transferred into 15 mL Falcon tubes and centrifuged for 3 minutes at 1200 rpm. The supernatant was collected and 1 mL of paraformaldehyde (PFA) 2 % in PBS was added to each tube, the samples were incubated at room temperature for 30 minutes and centrifuged again at 1200 rpm for 3 minutes to remove excess PFA. The pellet was resuspended in 1 mL of PBS after the supernatant was removed, the tubes were centrifuged again, and the pellet was resuspended in 350 µL of PBS. The cells were then examined by Flow Cytometry (BD – Accuri C6 Plus). To analyze the data obtained by the Flow Cytometer the FlowJo™ software was utilized, where it was calculated the geometric mean fluorescence intensity (GEO MFI) values of each treatment, which is the parameter used to evaluate the interaction the NPs had with the cells.

2.8. Detection of Variations on the Plasma Membrane in A549 Cells Using Laurdan and Two-Photon Excitation Microscopy

For this experiment, both f-NPs with p28 and nf-NPs were produced and characterized as described above, after making sure that both types of NPs were suitable for use, A549 cells were seeded on µ-Slide 8 well IBIDI glass bottom chambers (ibidi®) with $7.5x10^5$ cells and left to adhere and grow overnight in a CO_2 incubator (5 %) at 37 ℃. On the next day, the medium was collected, and the cells were incubated with Free p28 (2.5 µM and 50 µM), f-NPs (250 µg/mL), and nf-NPs (250 µg/mL). For control, the cells were incubated only with the medium. Cells were left for 4 h before 5 µM of the fluorescent dye Laurdan was added and the cells were incubated in a CO_2 incubator at 37 ℃ for 20 minutes. The experiments were analyzed on an inverted microscope (model no. DMI6000) of Leica TCS SP5 (Leica Microsystems CMS GmbH, Mannheim, Germany) with a 63x water (1.2-numerical-aperture) apochromatic objective. The data from the two-photon excitation microscopy was obtained with a Ti:sapphire laser (Mai Tai, Spectra-Physics, Darmstadt, Germany) as the excitation light source. The excitation wavelength was set to 780 nm and the fluorescence emission was collected at 400-460 nm and 470-530 nm to calculate the generalized polarization (GP) images. Laurdan GP images were analyzed through a homemade software called GPIMAGE based on a MATLAB (MathWorks) environment, with the GP value defined as:

$$GP = \frac{I_{400-460} - GI_{470-530}}{I_{400-460} + GI_{470-530}}$$

(Equation 3)

Where G is the calibration factor for the experimental setup, which is obtained from imaging Laurdan in dimethyl sulfoxide (DMSO) using the same experimental conditions as those set for the measurement in living cells [13]. At least 5 to 10 independent cells were analyzed per condition. The dark counts were subtracted from all intensity values and, in the analysis, only Regions of Interest (ROI) corresponding to the plasma membranes in each cell were selected, restricting, therefore, the analysis to this cellular component.

3. Results & Discussion

3.1. Interaction of p18 Peptide-functionalized Polymeric Nanoparticles with A549 and 16HBE14o- Cells

Firstly, p18 was conjugated with PLGA-PEG-Mal, and the resulting conjugate gave an efficiency conjugation of 69 % through an analysis by HPLC. After having this conjugate the production of NPs was made by the nanoprecipitation method, in which two samples were obtained, nf-NPs and f-NPs. These samples were characterized in terms of their physicochemical characteristics (Z-average, ζ-potential, and PDI) to confirm that both types of NPs are appropriate for testing on cells to compare the cell interaction of nf-NPs and f-NPs in cancer and normal cells by using Flow Cytometry.

Both A549 cells and 16HBE14o- cells were incubated with different concentrations of fluorescent f-NPs and nf-NPs. By analyzing the samples by flow cytometry, the fluorescent intensity is detected by the FL4 detector. After obtaining the fluorescence intensity values, the Geo MFI values of each treatment with f-NPs or nf-NPs were calculated with the FlowJo™ software to verify which type of NP interacted more with the cells. To see if there is indeed an advantage in using a smaller peptide, we compared the results of the flow cytometry of p18 to the results made by Garizo *et al*. [11] of p28. Starting with the interaction between the cell line A549 and the NPs with or without the acid wash (Figure 2A and 2B) we can observe that p18-NPs (f-NPs) had more interaction with the cells than the nf-NPs in every concentration,

which means that p18, just like p28, enhances the interaction of NPs with cells. However, p28-NPs had more interaction with the cells than p18-NPs in almost every concentration, with an exception on the interaction with acid wash in the concentrations 100 and 250 µg/mL, although not very significant. The identical happens with the interaction between the cell line 16HBE14o- and NPs with or without the acid wash. Once more, p18-NPs had more interaction than nf-NPs, but p28-NPs still had more interaction to the cells than p18-NPs (Figure 2C and 2D), which in this case it can be a good thing because we do not want NPs conjugated with CPPs entering the non-cancer human cells.

A

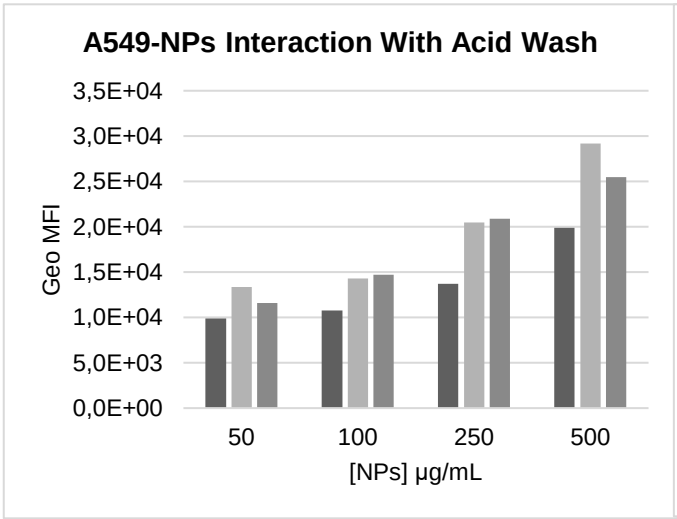

B

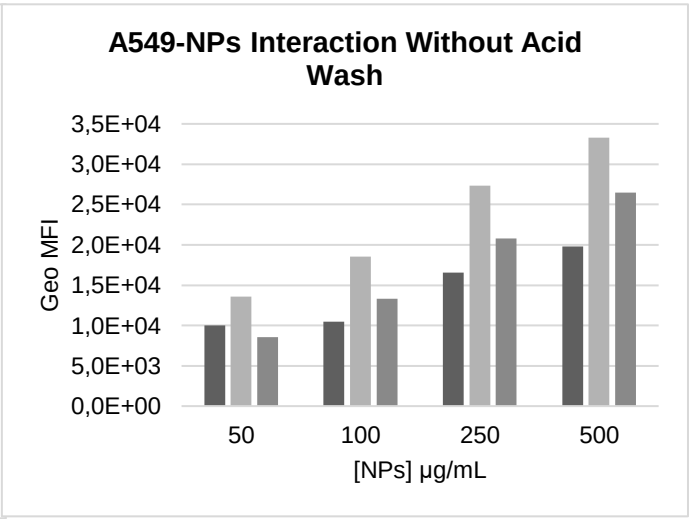

C

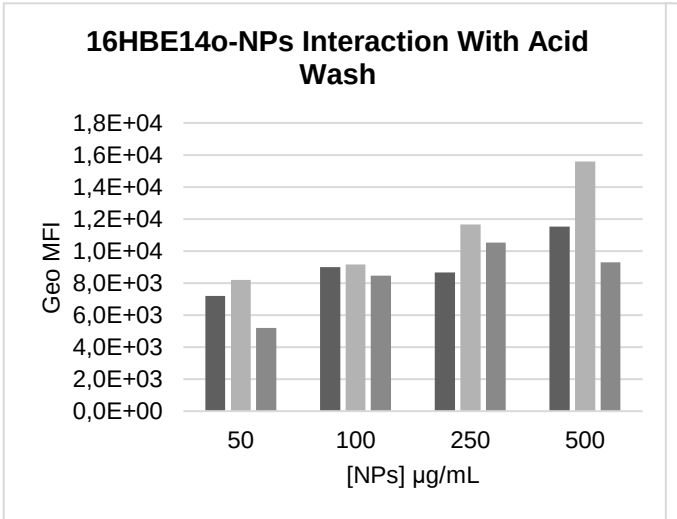

D

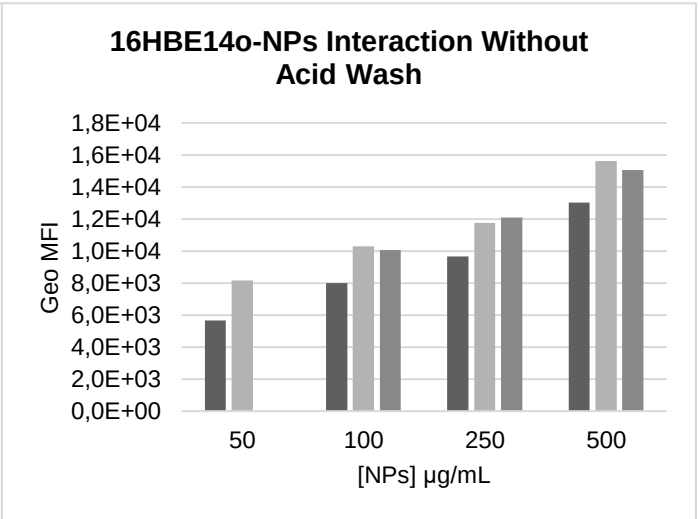

Figure 2 - (A) Comparison of Geo MFI values of A549 cells incubated with non-functionalized NPs and NPs functionalized with p18 and p28, with acid wash. (B) Comparison of Geo MFI values of A549 cells incubated with non-functionalized NPs and NPs functionalized with p18 and p28, without acid wash. (C) Comparison of Geo MFI values of 16HBE14o- cells incubated with non-functionalized NPs and NPs functionalized with p18 and p28, with acid wash. (D) Comparison of Geo MFI values of 16HBE14o- cells incubated with non-functionalized NPs and NPs functionalized with p18 and p28, without acid wash.

3.2. Detection of Variations on the Plasma Membrane in Cells using p28-NPs Nanosystems

It has already been observed that azurin protein and its peptide p28 leads to a decrease content of lipid raft components GM-1 and CAV1 [14]. Lipid rafts are present in the outer leaflet of the membranes and contains the combinations of specific lipids, cholesterol, and sphingolipids [14,15]. Evidence shows that changes in cholesterol metabolism is involved in carcinogenesis, since increased cholesterol levels are associated with a higher cancer incidence. Therefore, molecules that help reduce these high levels are beneficial because they reduce the risk and mortality of some cancers [16]. Having this in mind, the effects of four different treatments were evaluated in the organization of the plasma membrane in A549 cancer cells, by assessing the membrane fluidity with the fluorescent probe Laurdan. In this experiment the GP of Laurdan was measured to evaluate the lipid membrane hydration, because GP measures surface hydration of lipid membranes [17]. Higher GP values are associated to higher membrane ordering and a less fluid membrane.

Firstly, for this experiment, p28 was bound to PLGA-PEG-Mal the same way it is described above, which gave a conjugation efficiency of 78%. Then, the f-NPs and nf-NPs were produced by the nanoprecipitation method, but in this case without the fluorescent probe PLGA-FKR648. Their physicochemical proprieties were analyzed through DLS, and it was concluded that these NPs were suitable for experimentation. After incubating the A549 cells with the four different experimental conditions for 4 hours, the fluorescent probe Laurdan was incubated for 20 min, and then these cells were analyzed on an inverted microscope. As it can be observed in Figure 3, every condition tested caused a decrease in the GP values measured in the plasma membrane order when compared with the control. In Figure 3, is possible to observe that the results show that the fluidity of the plasma membrane increases after exposure to the treatments, as evaluated by changes in the Laurdan GP values. However, these results need to be interpreted cautiously as the method used is not very accurate and precise. Nevertheless, from our preliminary data it is possible to observe that the treatments which induced more fluidity of the plasma membrane are the ones with Free p28 peptide, especially with the lower concentration. One reason for this outcome could be that, as has been documented previously in the literature, at higher peptide concentrations uptake is caused by a mechanism that starts from spatially constrained locations of the plasma membrane and causes a rapid distribution of the peptides throughout the cytoplasm. Previous observations noted an absence of endocytic vesicles when cells are treated with higher concentrations of CPPs, suggesting an uptake mechanism independent of endocytosis. While in lower concentrations, endocytosis predominates [18,19]. Therefore, higher concentrations of the peptide may have less of an impact on the plasma membrane since they do not enter cells through endocytosis. However, more replicates of this procedure would be necessary to validate this hypothesis. Regarding the treatments with NPs, the nf-NPs treatment caused more disruption to the plasma membrane than the f-NPs, although not very marked, which was not an expected result since

the f-NPs are functionalized with p28. Therefore, it would be more expected for the latter to have caused a greater fluidity to the membrane, so, once again, more experiments would be needed. The reason why these 4 conditions have caused changes in the fluidity of the membrane of A549 cells may be that the entry of free p28 and p28-NPs is preferentially through caveolae/lipid rafts. Therefore, they most likely displaced Cav-1 from the membrane, at least temporarily, which disrupted the raft organization, likely affecting plasma membrane organization, and reducing the proportion of liquid-ordered membrane/domains. These findings are consistent with earlier findings from our group's studies, with the exception that in these studies azurin protein was utilized. The studies showed that azurin causes biophysical changes at the plasma membrane level, which attenuate signaling pathways involved in motility, adhesion, and invasiveness [15].

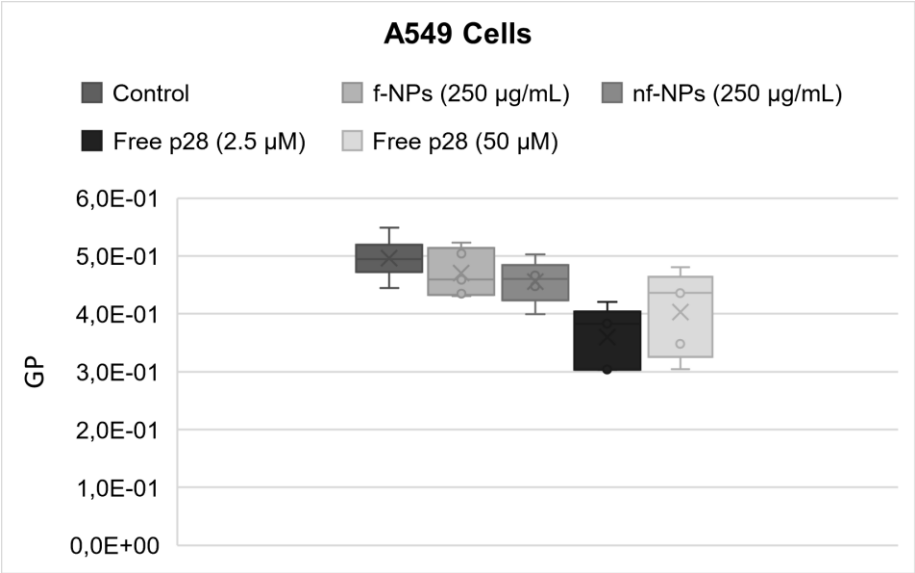

Figure 3 – Average GP values obtained for cells after incubation with functionalized NPs (f-NPs) and non-functionalized NPs (nf-NPs) at 250 µg/mL, and free p28 peptide at 2.5 µM and 50 µM are shown for the plasma membrane of A549 human cancer cell line. Every experiment causes a decrease in the average GP value, after 4 hours, when compared with the control. Average GP values are expressed as mean ± SD from at least 5 to 10 individual cells in each condition.

4. Conclusion

Nanotechnology has been intensively studied in the past years showing a huge potential for cancer therapy, especially due to the NPs used which have a size scale adequate to enter living human cells. NPs, when utilized as drug delivery molecules, have shown promise to increase the efficacy and safety of cancer therapies, however, improved delivery and a more specific targeting to cancer cells is needed. A way to obtain this is by functionalizing NPs with targeting ligands displayed at their surface, such as CPPs. The first objective of this current work was a follow up of the work previously made by our group [11], with a small change on the CPP that instead of using the full p28 peptide sequence, a smaller version of that peptide called p18 was used. The only difference between these two peptides is the inexistence of the domain responsible for the cytotoxicity activity. Therefore, the other domain, responsible for the preferential entry of p18, was studied. Firstly, p18 was conjugated to

PLGA-PEG-Mal which gave a conjugation efficiency of 69 % by analyzing the PLGA-PEG-Mal-p18 supernatants through HPLC. After that, p18-functionalized and non-functionalized PLGA-NPs with known properties were formulated and exposed to cells for a flow cytometry analysis. The results from flow cytometry were compared to previous data of p28-functionalized NPs and indicate that p18-NPs and p28-NPs both have a higher specificity to lung cancer cells than bronchial non-cancer cells. However, p18 did not demonstrate a higher specificity to cells than p28. So, overall, this peptide did not demonstrate advantages in terms of interacting more with the A549 human cancer cell line, thus it will not be used for now in upcoming work.

The peptide p28 was conjugated to PLGA-PEG-Mal for the second objective of this thesis in the same manner as p18, with a conjugation efficiency of 78 %. After that, PLGA-NPs with and without p28 functionalization were created, and DLS confirmed they have the physicochemical properties needed for future testing. To identify the possible effects at the plasma membrane using the fluorescent probe Laurdan, both types of NPs were incubated with A549 cancer cells, as well as the free unconjugated p28 (2.5 μM and 50 μM). It has already been noted that the azurin protein and its peptide, p28, can lower the levels of the lipid raft components GM-1 and CAV1, increase membrane fluidity, and encourage endocytosis [14]. The same observations were made in this work. In all four experimental conditions used here, a decrease in the membrane order was observed, with free p28 at the lowest concentration showing the most significant effect. In addition, both non-functionalized and functionalized NPs exhibited the same behavior, however, no differences were observed regarding the presence of p28 at the surface of the NPs. It may be that, although cells may uptake NPs by endocytosis which induces the differences observed related to the control, the levels of p28 present in there may not be enough for the changes to be observed by this technique. So, in conclusion, this suggests that targeting cancer cells by acting at the membrane level may be a novel approach, opening the possibility of developing novel treatment approaches and drug delivery systems based on their activities, which may improve the absorption and efficiency of other medications.

5. References

1. Zhao CY, Cheng R, Yang Z, Tian ZM. Nanotechnology for Cancer Therapy Based on Chemotherapy. *Molecules*. 2018;23(4):826. doi:10.3390/molecules23040826

2. Saxena SK, Khurana SMP, eds. *NanoBioMedicine*. Springer Singapore; 2020. doi:10.1007/978-981-32-9898-9

3. Jin C, Wang K, Oppong-Gyebi A, Hu J. Application of Nanotechnology in Cancer Diagnosis and Therapy - A Mini-Review. *Int J Med Sci*. 2020;17(18):2964-2973. doi:10.7150/ijms.49801

4. Heinz H, Pramanik C, Heinz O, et al. Nanoparticle decoration with surfactants: Molecular interactions, assembly, and applications. *Surface Science Reports*. 2017;72(1):1-58. doi:10.1016/j.surfrep.2017.02.001

5. Derakhshankhah H, Jafari S. Cell penetrating peptides: A concise review with emphasis on biomedical applications. *Biomedicine & Pharmacotherapy*. 2018;108:1090-1096. doi:10.1016/j.biopha.2018.09.097

6. Kamp M, Silvestrini MC, Brunori M, Beeumen J, Hali FC, Canters GW. Involvement of the hydrophobic patch of azurin in the electron-transfer reactions with cytochrome c551 and nitrite reductase. *Eur J Biochem*. 1990;194(1):109-118. doi:10.1111/j.1432-1033.1990.tb19434.x

7. Huang F, Shu Q, Qin Z, et al. Anticancer Actions of Azurin and Its Derived Peptide p28. *Protein J*. 2020;39(2):182-189. doi:10.1007/s10930-020-09891-3

8. Yamada T, Fialho AM, Punj V, Bratescu L, Gupta TKD, Chakrabarty AM. Internalization of bacterial redox protein azurin in mammalian cells: entry domain and specificity: Entry domain of azurin. *Cellular Microbiology*. 2005;7(10):1418-1431. doi:10.1111/j.1462-5822.2005.00567.x

9. Yamada T, Christov K, Shilkaitis A, et al. p28, A first in class peptide inhibitor of cop1 binding to p53. *Br J Cancer*. 2013;108(12):2495-2504. doi:10.1038/bjc.2013.266

10. Yaghoubi A, Khazaei M, Avan A, Hasanian SM, Cho WC, Soleimanpour S. p28 Bacterial Peptide, as an Anticancer Agent. *Front Oncol*. 2020;10:1303. doi:10.3389/fonc.2020.01303

11. Garizo AR, Castro F, Martins C, et al. p28-functionalized PLGA nanoparticles loaded with gefitinib reduce tumor burden and metastases formation on lung cancer. *Journal of Controlled Release*. 2021;337:329-342. doi:10.1016/j.jconrel.2021.07.035

12. Sato AK, Viswanathan M, Kent RB, Wood CR. Therapeutic peptides: technological advances driving peptides into development. *Current Opinion in Biotechnology*. 2006;17(6):638-642. doi:10.1016/j.copbio.2006.10.002

13. Owen DM, Rentero C, Magenau A, Abu-Siniyeh A, Gaus K. Quantitative imaging of membrane lipid order in cells and organisms. *Nat Protoc*. 2012;7(1):24-35. doi:10.1038/nprot.2011.419

14. Bernardes N, Garizo AR, Pinto SN, et al. Azurin interaction with the lipid raft components ganglioside GM-1 and caveolin-1 increases membrane fluidity and sensitivity to anti-cancer drugs. *Cell Cycle*. 2018;17(13):1649-1666. doi:10.1080/15384101.2018.1489178

15. Bernardes N, Fialho A. Perturbing the Dynamics and Organization of Cell Membrane Components: A New Paradigm for Cancer-Targeted Therapies. *IJMS*. 2018;19(12):3871. doi:10.3390/ijms19123871

16. Ding X, Zhang W, Li S, Yang H. The role of cholesterol metabolism in cancer. *Am J Cancer Res.* February 1, 2019:219-227.

17. Nishida K, Nishimura S nosuke, Tanaka M. Selective Accumulation to Tumor Cells with Coacervate Droplets Formed from a Water-Insoluble Acrylate Polymer. *Biomacromolecules*. 2022;23(4):1569-1580. doi:10.1021/acs.biomac.1c01343

18. Duchardt F, Fotin-Mleczek M, Schwarz H, Fischer R, Brock R. A Comprehensive Model for the Cellular Uptake of Cationic Cell-penetrating Peptides. *Traffic*. 2007;8(7):848-866. doi:10.1111/j.1600-0854.2007.00572.x

19. Ruseska I, Zimmer A. Internalization mechanisms of cell-penetrating peptides. *Beilstein J Nanotechnol*. 2020;11:101-123. doi:10.3762/bjnano.11.10